

Supporting Information

Facile Synthesis of a Mesoporous Benzothiadiazole-COF Based on a Transesterification Process

Mirjam Dogru, Andreas Sonnauer, Silvia Zimdars, Markus Döblinger, Paul Knochel* and Thomas Bein*

Department of Chemistry and Center for NanoScience (CeNS) Ludwig-Maximilians-Universität Munich(LMU)Butenandtstraße 5–13, 81377 München Germany

Fax: (+49) 89-2180-77622

E-mail: bein@lmu.de, knoch@cup.uni-muenchen.de

Homepage <http://www.bein.cup.uni-muenchen.de>

1. Materials and Methods

All materials (if not otherwise noted) were purchased from Aldrich or Fluka in the common purities purum and puriss. All materials were used without further purification.

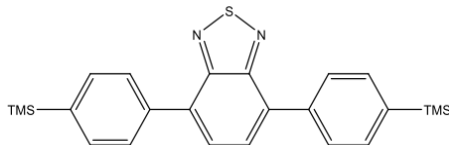
X-ray diffraction analysis was carried out in reflection mode using a Bruker D8 Discover with Ni-filtered $\text{CuK}\alpha$ -radiation (1.5406 Å) and a position-sensitive detector (Vantec). Fourier-transform infrared spectra of the samples were measured with a Bruker Equinox 55 equipped with a PIKE MIRacle ATR-unit at room temperature. Transmission electron microscopy data were obtained with a FEI Titan 80-300 microscope at an acceleration voltage of 80 kV. ^{11}B and ^{13}C MAS NMR spectra were recorded on a Bruker DSX Avance 500 with a magnetic field of 11.2 Tesla. A 4 mm MAS triple-resonance sample head was used. ^{11}B -NMR spectra were recorded with single pulse program with 90 scans and a delay time of 1 sec. For ^{13}C -CP-MAS-NMR 1808 scans were performed and with delay time of 2 sec. The frequency of the rotors was 10 kHz. TG measurements were performed in a stream of synthetic air (25 ml/min) on a Netzsch STA 440 C TG/DSC. The measurements were carried out with a heating rate of 10 K/min and a temperature range from 30 °C to 900 °C. Nitrogen sorption isotherms were recorded on a Nova 4000e at 77 K. Prior to the measurement of the adsorption isotherm the sample was heated for 12 h at 200 °C under oil pump vacuum. The calculation of the pore size distribution was done using the NLDFT model with a carbon kernel for cylindrical pores, using the desorption branch.

Molecular geometry optimization was performed with Accelrys MS Modeling 4.4 using the universal force field method. The final hexagonal unit cell was calculated with the geometrical parameters from the optimized structure. For the simulation of the PXRD pattern Reflex was used (a software package implemented in MS Modeling 4.4). For this purpose the unit cell parameters were first calculated and then refined from the experimentally observed peak positions in a hexagonal array. As a result we obtained cell parameters of $a = b = 44.29$ Å and $c = 3.53$ Å. The simulated PXRD patterns were then compared with the experimentally obtained data. We note that this structure can assemble in two different arrangements, i.e., (i) a staggered AB type with graphite-like packing, and (ii) an eclipsed AA type arrangement with the adjacent sheets lying exactly on top of each other. After optimizing the geometry of each arrangement, the powder patterns were simulated and compared to the experimental patterns. The simulated pattern of the AA arrangement shows very good agreement with our experimental PXRD pattern.

2. Synthesis

Synthesis of 4,7-Bis(4-(trimethylsilyl)phenyl)benzo[c][1,2,5]thiadiazole (3)

The starting materials benzo[c][1,2,5]thiadiazole and dibromobenzo[c][1,2,5]thiadiazole were synthesized following published procedures.^{1,2}



In a 250 mL Schlenk-flask equipped with a stirring bar under argon atmosphere bis(di-*tert*-butyl(4-dimethylaminophenyl)phosphine)dichloropalladium(II) (28 mg, 0.04 mmol) and 4,7-dibromobenzo[c][1,2,5]thiadiazole (1.47 g, 5 mmol) were added successively to a solution of 4-(trimethylsilyl)phenylzinc(II) chloride (36.4 mL of a 0.55 M solution in THF, 20 mmol) and the resulting greenish reaction mixture was stirred at 50 °C for 3 h. After addition of 100 mL saturated NH₄Cl solution the aqueous layer was extracted with CH₂Cl₂ (3 times 200 mL). The combined organic layers were dried with MgSO₄ and the solvents evaporated in vacuo. Purification via column separation (silicagel, pentane) yielded 4,7-bis(4-(trimethylsilyl)phenyl)benzo[c][1,2,5]thiadiazole (**3**) (1.6 g, 75 %) as a bright yellow solid.

mp (°C): 151.1–152.8.

IR (ATR) $\tilde{\nu}$ (cm⁻¹): 3016 (w), 2952 (w), 2894 (w), 1554 (w), 1480 (w), 1400 (w), 1247 (m), 1095 (w), 837 (vs), 818 (s), 813 (s), 757 (m), 721 (m), 691 (w).

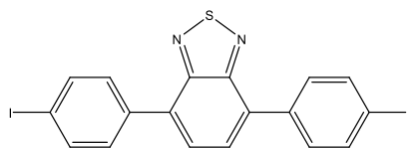
¹H-NMR (300 MHz, CDCl₃): δ = 7.96–7.92 (m, 4H), 7.79 (s, 2H), 7.73–7.70 (m, 4H), 0.34 ppm (s, 18H).

¹³C-NMR (75 MHz, CDCl₃): δ = 154.2, 140.8, 137.8, 133.7, 133.5, 128.5, 128.1, –1.1 ppm.

MS (70 eV, EI): *m/z* (%) = 434 (10), 433 (32), 432 (79), 419 (17), 418 (40), 417 (100), 202 (14), 201 (35), 73 (18), 57 (10).

HRMS (EI): *m/z* calc. for [C₂₄H₂₈N₂SSi₂] 432.1512; found: 432.1509.

Synthesis of 4,7-Bis(4-iodophenyl)benzo[c][1,2,5]thiadiazole (4)



In a 500 mL round bottom flask 4,7-Bis(4-(trimethylsilyl)phenyl)benzo[c][1,2,5]thiadiazole (10 g, 23 mmol) was dissolved in 200 mL CH₂Cl₂ and cooled to 0 °C. ICl (2 mL, excess) was added dropwise and the reaction mixture stirred at 0 °C for 10 min, slowly warmed up to 20 °C and stirred for further 2 h. Filtration yielded 4,7-bis(4-iodophenyl)benzo[c][1,2,5]thiadiazole (**4**) (11.6 g, 93 %) as a yellow solid.

mp (°C): 214.0–217.8.

IR (ATR) $\tilde{\nu}$ (cm⁻¹): 2920 (w), 2851 (w), 1586 (w), 1552 (w), 1472 (m), 1402 (w), 1116 (w), 1102 (w), 1060 (w), 1006 (m), 972 (w), 943 (w), 886 (w), 849 (w), 806 (vs), 710 (w).

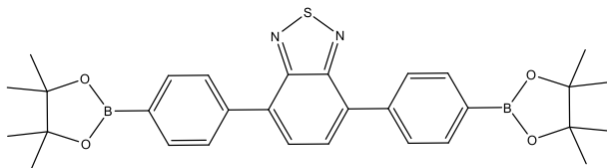
¹H-NMR (300 MHz, CDCl₃): δ = 7.90–7.85 (m, 4H), 7.76 (s, 2H), 7.73–7.68 ppm (m, 4H).

¹³C-NMR (75 MHz, CDCl₃): δ = 153.8, 137.8, 136.7, 132.6, 131.0, 127.9, 94.6 ppm.

MS (70 eV, EI): m/z (%) = 542 (6), 541 (21), 540 (100), 288 (11), 286 (9), 143 (6).

HRMS (EI): m/z calc. for [C₁₈H₁₀I₂N₂S] 539.8654; found: 539.8650.

Synthesis of 4,7-Bis(4-(4,4,5,5-tetramethyl-1,3,2-dioxaborolan-2-yl)phenyl)benzo-[c][1,2,5]-thiadiazole (1)



In a 250 mL Schlenk-flask equipped with a stirring bar KOAc (4.9 g, 50 mmol) was dried under 10^{-5} bar at 100 °C. After addition of 100 mL 1,4-dioxane, 4,7-bis(4-iodophenyl)benzo[c][1,2,5]thiadiazole (5.4 g, 10 mmol) and 4,4,4',4',5,5,5',5'-octamethyl-2,2'-bi(1,3,2-dioxaborolane) (10.2 g, 40 mmol) the reaction mixture was degassed. Pd(OAc)₂ (90 mg, 0.4 mmol) and tricyclohexylphosphine (220 mg, 0.8 mmol) were added successively and the resulting greenish reaction mixture stirred at 80 °C for 24 h. After addition of 100 mL saturated NaHCO₃ solution the aqueous layer was extracted with Et₂O (4 times 200 mL). The combined organic layers were dried with MgSO₄ and the solvents evaporated in vacuo. Recrystallization from Et₂O yielded 4,7-Bis(4-(4,4,5,5-tetramethyl-1,3,2-dioxaborolan-2-yl)phenyl)benzo[c][1,2,5]thiadiazole (**1**) (4.1 g, 74 %) as a bright yellow solid.

mp (°C): 184.0–186.2.

IR (ATR) $\tilde{\nu}$ (cm⁻¹): 2975 (w), 1609 (w), 1550 (w), 1519 (w), 1396 (m), 1356 (vs), 1320 (m), 1294 (m), 1214 (w), 1143 (s), 1122 (m), 1105 (m), 1084 (m), 1020 (w), 961 (w), 890 (w), 856 (m), 821 (s), 744 (w), 657 (m).

¹H-NMR (600 MHz, CDCl₃): δ = 8.00–7.95 (m, 8H), 7.80 (s, 2H), 1.37 ppm (s, 24H).

¹³C-NMR (150 MHz, CDCl₃): δ = 154.0, 140.0, 135.0, 133.5, 128.5, 128.2, 83.9, 24.9 ppm.

MS (70 eV, EI): m/z (%) = 542 (10), 541 (34), 540 (100), 539 (44), 441 (14), 440 (11), 341 (24), 340 (22), 339 (9).

HRMS (EI): m/z calc. for [C₃₀H₃₄B₂N₂O₄S] 540.2425; found: 540.2419.

Synthesis of BTD-COF

BTD-COF was synthesized starting from 4,7-bis[4-(4,4,5,5)-tetramethyl-[1,3,2]dioxaborolan-2-yl]-phenyl]-benzo[1,2,5]thiadiazole (BTDBE) and 2,3,6,7,10,11-hexahydroxyphenylene (HHTP) in a two step synthesis by microwave heating. The syntheses were performed in special microwave vials 0.5-2 ml from Biotage. In step 1 BTDBE (32.4 mg, 0.06 mmol) was dissolved in a mixture of 1,4-dioxane/mesitylene (375 μ L / 375 μ L), and concentrated HCl (37 wt-%, 105 μ L) was added. The mixture was heated up to 180 °C for 10 minutes under continuous stirring (600 rpm). A phase mixture of a yellow precipitate and solvents is obtained, which is necessary for reaction step 2. HHTP (13.0 mg, 0.04 mmol) and a mixture of 1,4-dioxane/mesitylene (375 μ L / 375 μ L) was further added. The mixture was then heated for 30 minutes und continuous stirring at 160 °C to finally obtain a green powder (BTD-COF) with a yield based on BTDBE of about 75 Elemental Analysis calculated for C₉₀N₆O₁₂B₆H₄₂S₃: C, 69.10; H, 2.96; N, 5.37 and S: 6.15. Found: C, 65.14; H, 3.36; N, 4.31 and S, 4.87. Reference one-pot investigations for direct transesterification of BTDBE with HHTP were performed with microwave and conventional heating, but did not lead to the desired BTD-COF. The yellow precipitate after step 1 was also characterized by X-ray powder diffraction and revealed a crystalline phase, which could not be clearly identified, presumably a pre-condensed oligomer. Without this crystalline precursor no BTD-COF is formed during the reaction step 2. The BTD-COF is stable in most organic solvents, such as ethanol, acetone, acetonitrile, dichloromethane, chloroform and toluene.

The optimum reaction time and temperature for each of the two-steps were optimized by systematic parameter screening (Figure S1). The evaluation was based on crystallinity and yield of the obtained BTD-COF.

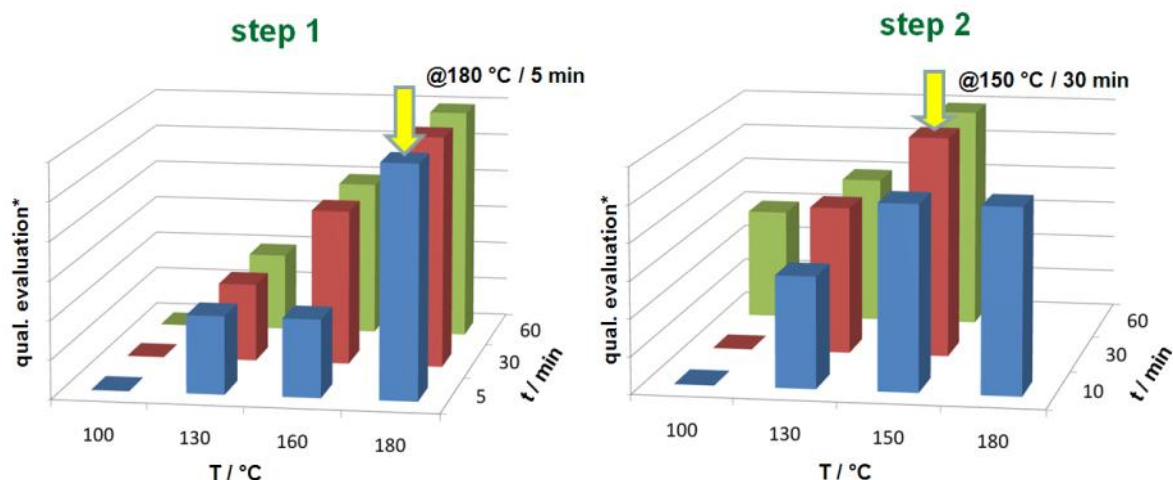


Figure S1: Optimization of step 1 (left) and step 2 (right). *Evaluation based on comparable crystallinity and yield of the products.

3. Simulation of the crystal structure of BTD-COF

Based on the functional groups and geometry of the used precursor molecules, the final structure can be predicted and then confirmed with experimental powder X-ray diffraction (PXRD). Based on the used precursor molecules a two-dimensional layered structure with hexagonal crystal system is expected. After comparison of simulated and measured PXRD the simulated structure could be verified. The structure was constructed with the visualization environment of Materials Studio, and the geometry of the two-dimensional layers was optimized by calculations using force field methods. The cell parameter a was adjusted from experimental PXRD results and was found to agree with the dimensions of the corresponding crystals determined by TEM. A precise determination of the c parameter from PXRD is difficult due to the low intensity of the (001) reflection. The simulation result was then finally compared to experimental PXRD data.

Crystal lattice

Table S1: Refined Crystal Data

Formula	$C_{90} N_6 O_{12} B_6 H_{42} S_3$
Formula weight	1560.42 g/mol
Crystal system	Hexagonal
Space group	P -62m
Unit cell dimensions	$a = b = 44.229 \text{ \AA}$ $c = 3.53 \text{ \AA}$
Cell Volume	5950.27 \AA^3

Table S2: Fractional atomic coordinates:

Atom	Wyck.	x	y	z
------	-------	---	---	---

C1	6k	0.46353	0.48148	0.50
C6	6k	0.40560	0.53906	0.50
C5	6k	0.42313	0.52115	0.50
N1	6k	0.42981	0.46049	0.50
O1	6k	0.36860	0.57506	0.50
C11	6k	0.46592	0.54266	0.50
C12	6k	0.33333	0.63380	0.50
C10	6k	0.36528	0.33223	0.50
C3	6k	0.53647	0.33333	0.50
C8	6k	0.59440	0.37468	0.50
C9	6k	0.57687	0.57219	0.50
O2	6k	0.63140	0.51839	0.50
C14	6k	0.66584	0.49389	0.50
C13	6k	0.66666	0.60380	0.50
C15	6k	0.63472	0.51852	0.50
C2	6k	0.03809	0.46094	0.50
C7	6k	0.15033	0.47885	0.50
C4	6k	0.07791	0.42494	0.50
B1	6k	0.40626	0.39803	0.50
C6H	6k	0.37542	0.36620	0.50
C5H	6k	0.40787	0.39620	0.50
C11H	6k	0.30827	0.51905	0.50
C3H	6k	0.56665	0.57517	0.50
C8H	6k	0.62458	0.53895	0.50
C9H	6k	0.59213	0.59374	0.50
C14H	6k	0.69173	0.52413	0.50
S1	3g	0.41520	0.49096	0.50

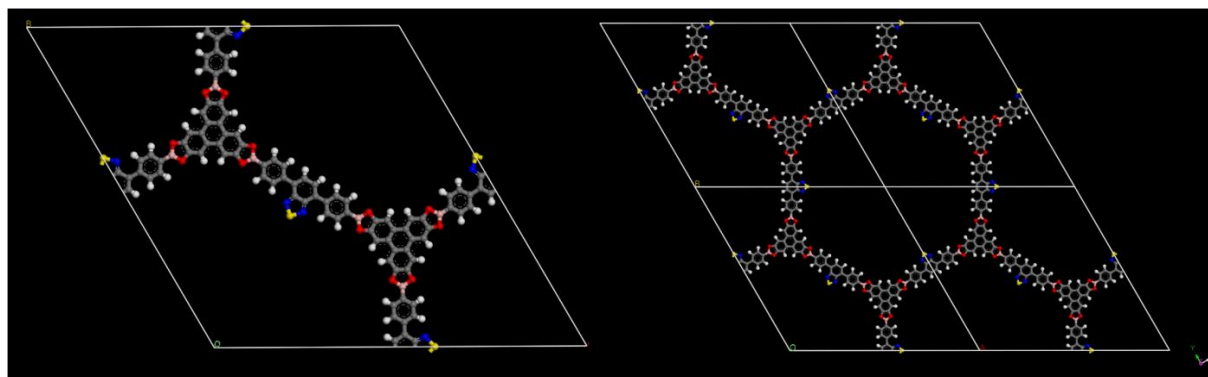


Figure S2: Simulation of the crystal lattice calculated in an eclipsed arrangement with cell parameter $a=b= 44.229 \text{ \AA}$; left: of one unit cell, right: of 4 unit cells.

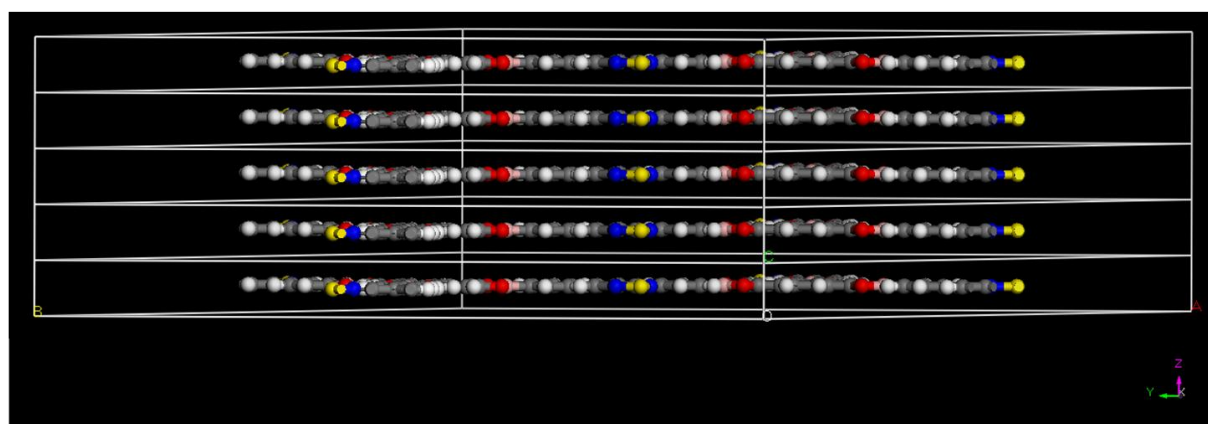


Figure S3: Simulation of the crystal lattice calculated in an eclipsed arrangement with a view along the c-axis with an interlayer distance of 3.53 \AA .

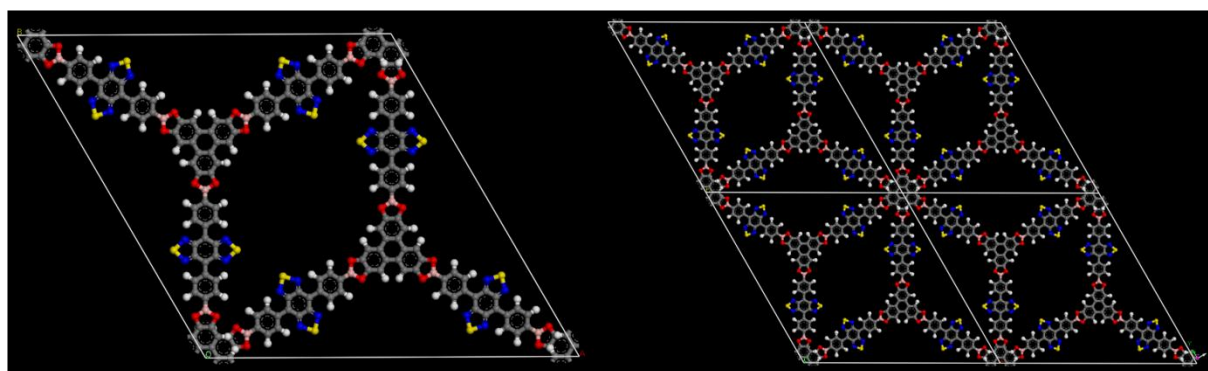


Figure S4: Simulation of crystal lattice calculated in a staggered arrangement (space group $P63/mmc$), left: view on AB plane of one unit cell, right: of four unit cells. The pore size and the internal surface area are both significantly smaller than the experimental data.

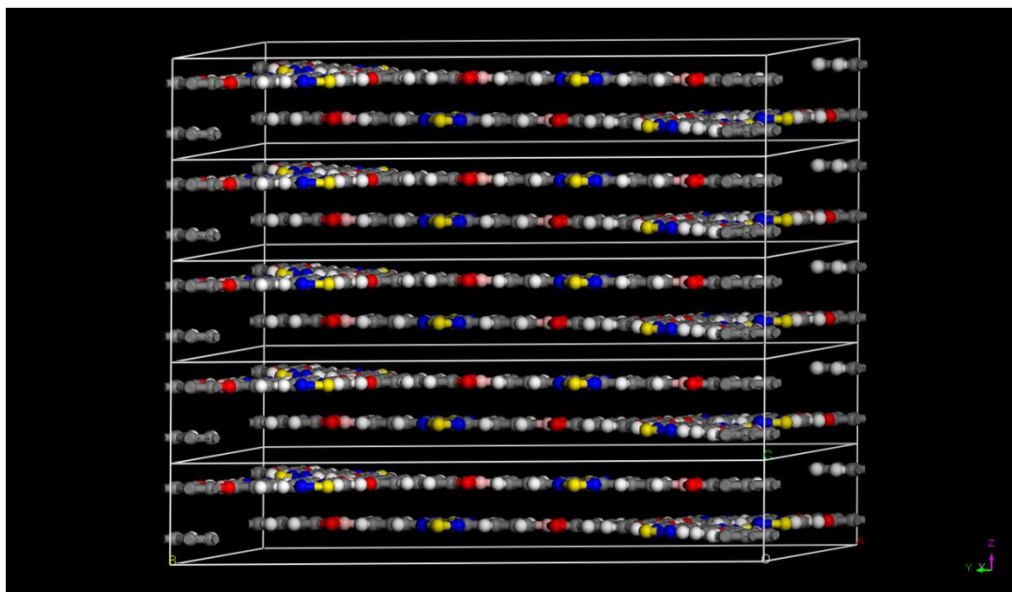


Figure S5: Simulation of crystal lattice in a staggered arrangement with a view along the c-axis. Doubling of the sheets leads to a larger interlayer distance of A-A, thus to a larger unit cell in the c direction, this would result a much smaller 2 theta value for the 001 reflection.

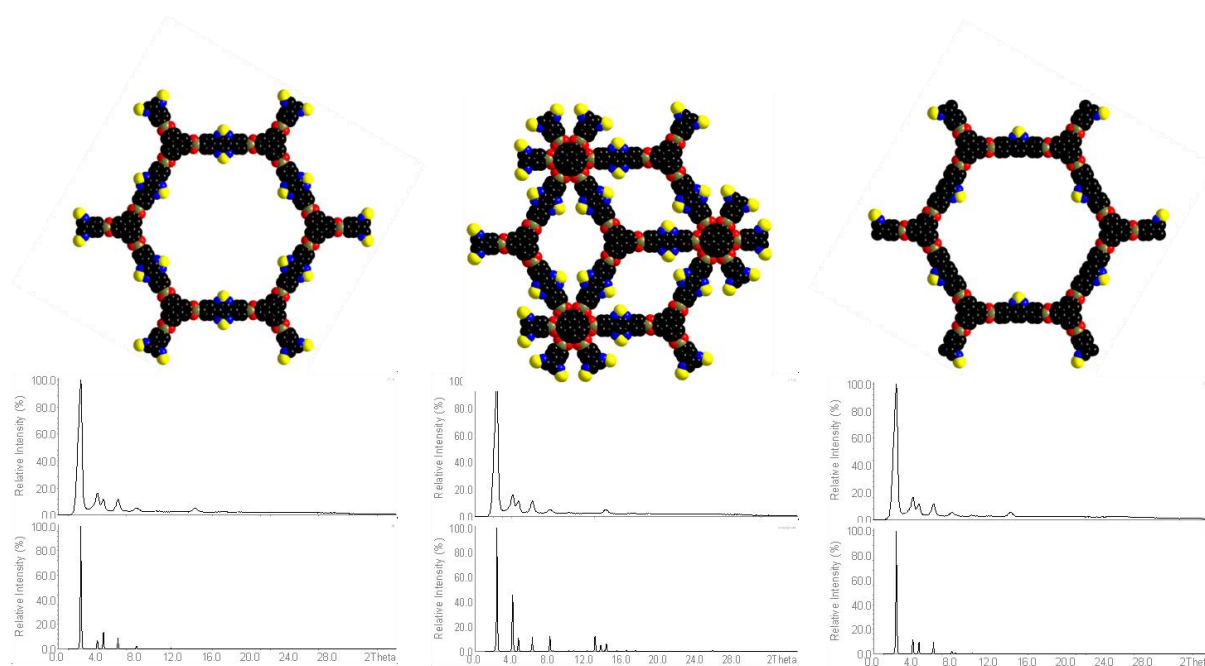


Figure S6: Comparison of different crystal structures of the BTD-COF with simulations of the XRD patterns in different space groups. Left: the benzothiadiazole group was placed on both sides of the corresponding aromatic ring with 50 % occupancy for a statistical arrangement resulting in a P6/mmm space group, middle: simulation in a staggered conformation (P63/mmc), right: calculation in the space group P-62m with alternating BTD-moieties gives the best fit.

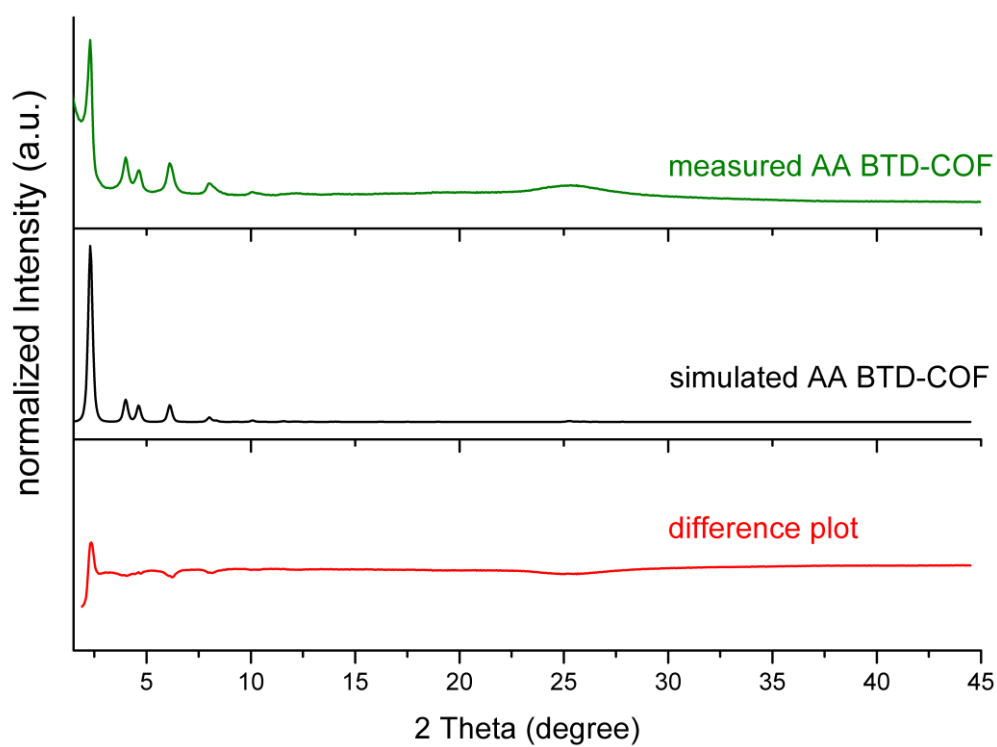


Figure S7: Difference plot of simulated diffraction data of BTD-COF in the eclipsed arrangement and experimental PXRD.

4. FT-IR Spectroscopy

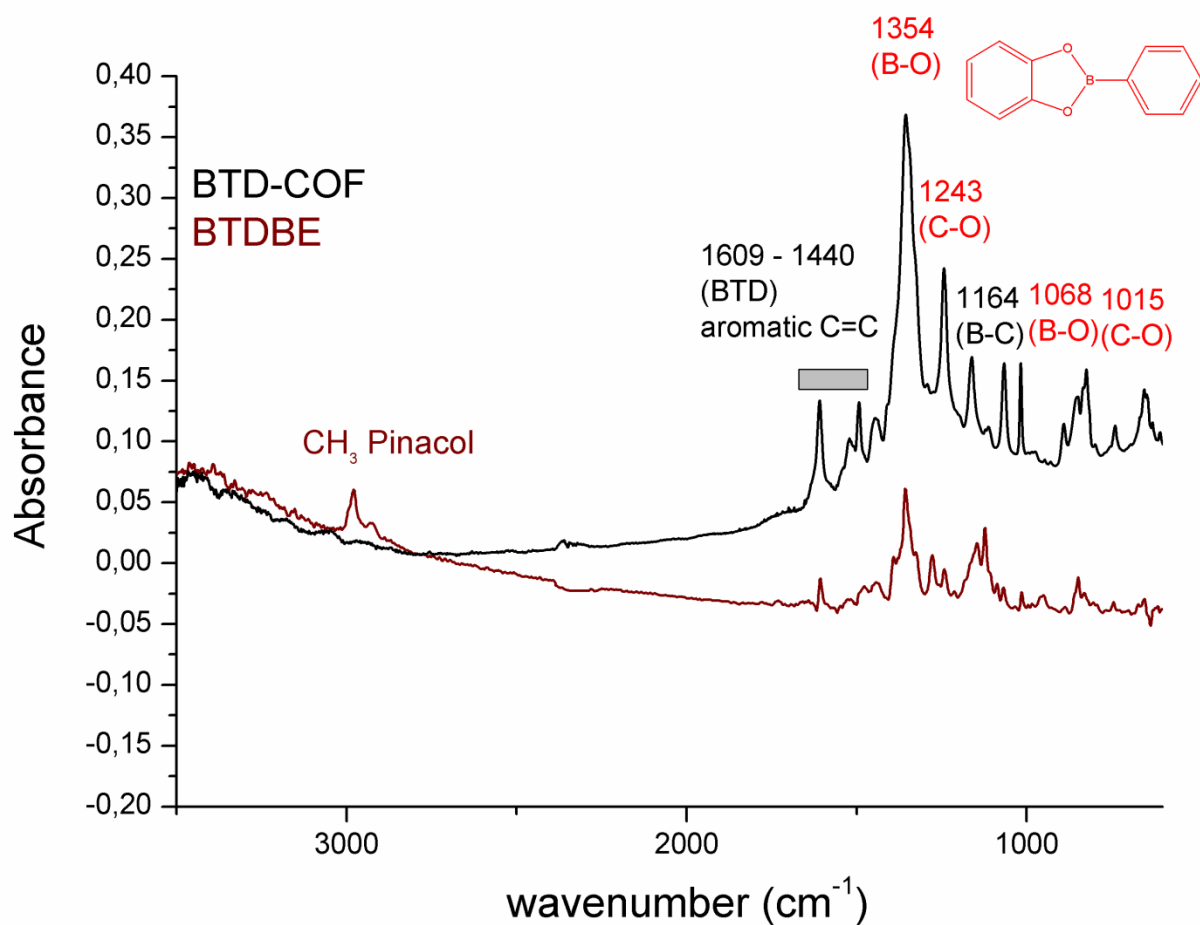


Figure S8: IR spectrum of BTD-COF (black) and the starting material BTDBE (red) with indication of the most important signals.

Table S 3: Assignment of the most important IR-bands of BTD-COF.

Peak (cm^{-1})	Assignment
3500 (m)	ν_{sym} OH from terminal OH and $\text{B}(\text{OH})_2$ groups
1603(m)	ν_{sym} C=C for phenanthrenes
1532(m)	
1489(m)	ν_{sym} C=C for aromatics
1354(s)	ν_{asym} B-O
1243(m)	ν_{asym} C-O
1164(m)	ν_{sym} B-C
1068 (m)	ν_{sym} B-O
1015 (m)	ν_{sym} C-O

5. MAS Nuclear Magnetic Resonance

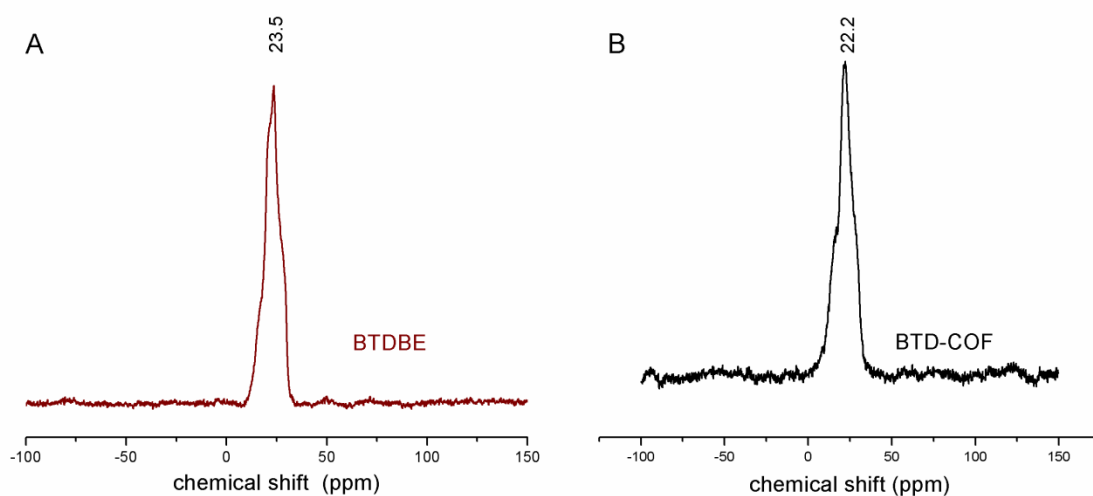


Figure S9: ^{11}B MAS-NMR spectrum of A) the starting material BTDBE (1) compared to B) BTD-COF.

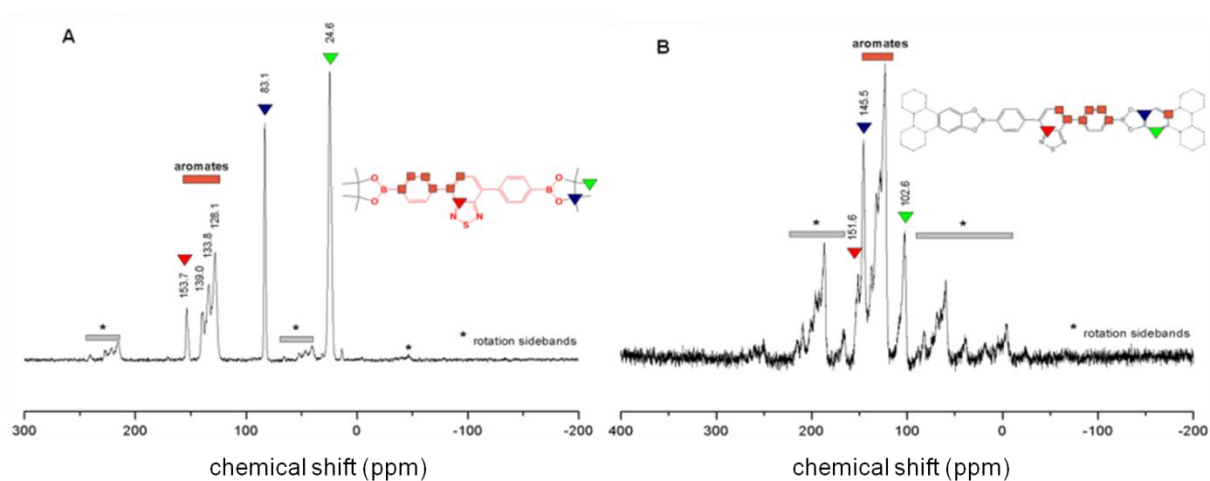


Figure S10: ^{13}C MAS-NMR of A) starting compound BTDBE (1) compared to B) BTD-COF.

6. Thermogravimetric Analysis

Thermogravimetric analysis indicates that BTD-COF is stable up to 450 °C. Heating to 200 °C is accompanied by a mass loss of 10%, which can be attributed to guest molecules in the mesopores. At 700 °C a total weight loss of 78% is reached. The remaining 12% correspond to the stoichiometrically expected amount of B_2O_3 .

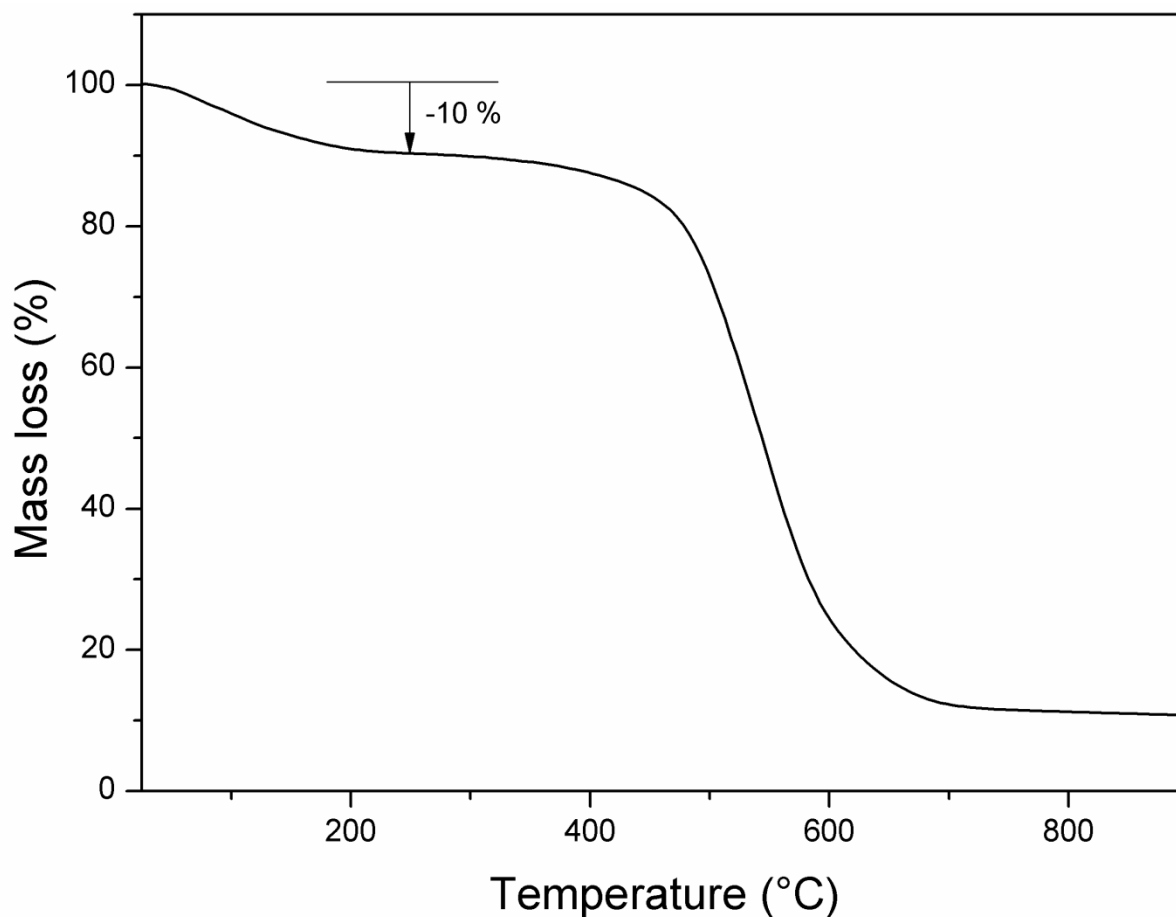


Figure S11: TG data for BTD-COF.

7. Fluorescence Spectra

Upon excitation at 330 nm, the BTD-COF showed fluorescence emission at 484 nm. Compared to the starting material, however, the fluorescence intensity was significantly lower.

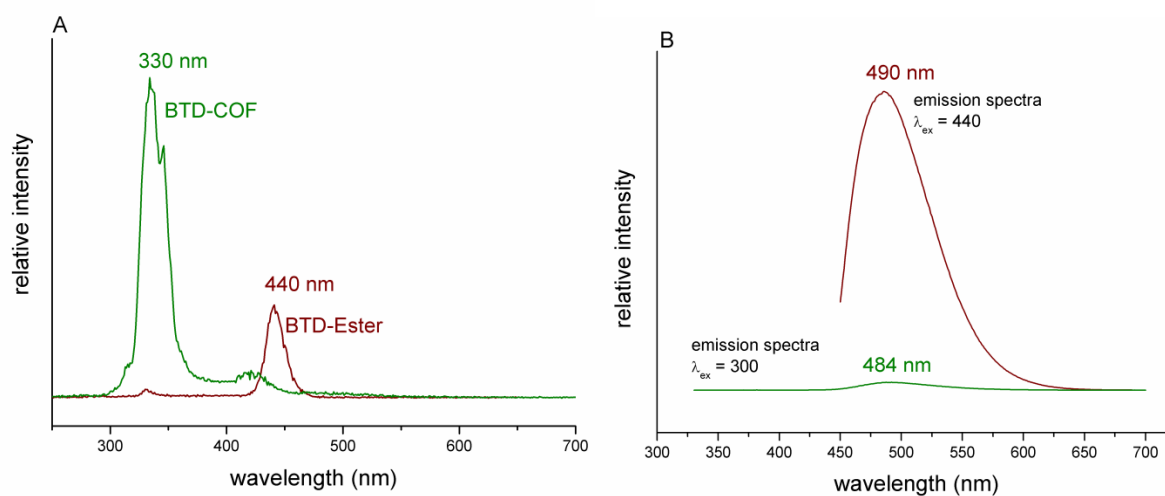


Figure S12: Fluorescence excitation (A) and emission (B) profiles of the starting pinacolboronate BTDBE (dark red) and the BTD-COF (green).